NRC Publications Archive
Archives des publications du CNRC

Laser-ultrasonic inspection of cold spray additive manufacturing components

Lévesque, Daniel; Bescond, Christophe; Cojocaru, Cristian

This publication could be one of several versions: author’s original, accepted manuscript or the publisher’s version. / La version de cette publication peut être l’une des suivantes : la version prépublication de l’auteur, la version acceptée du manuscrit ou la version de l’éditeur.
For the publisher’s version, please access the DOI link below./ Pour consulter la version de l’éditeur, utilisez le lien DOI ci-dessous.

Publisher’s version / Version de l'éditeur:
https://doi.org/10.1063/1.5099730
Review of Progress in Quantitative Nondestructive Evaluation, 38, pp. 020026-1-020026-10, 2019-05-08

NRC Publications Archive Record / Notice des Archives des publications du CNRC :
https://nrc-publications.canada.ca/eng/view/object/?id=15bdfd4e-0573-4c3f-86a9-282a2dfa4941
https://publications-cnrc.canada.ca/fra/voir/objet/?id=15bdfd4e-0573-4c3f-86a9-282a2dfa4941

Access and use of this website and the material on it are subject to the Terms and Conditions set forth at
https://nrc-publications.canada.ca/eng/copyright
READ THESE TERMS AND CONDITIONS CAREFULLY BEFORE USING THIS WEBSITE.

L’accès à ce site Web et l’utilisation de son contenu sont assujettis aux conditions présentées dans le site
https://publications-cnrc.canada.ca/fra/droits
LISEZ CES CONDITIONS ATTENTIVEMENT AVANT D’UTILISER CE SITE WEB.

Questions? Contact the NRC Publications Archive team at
PublicationsArchive-ArchivesPublications@nrc-cnrc.gc.ca. If you wish to email the authors directly, please see the first page of the publication for their contact information.

Vous avez des questions? Nous pouvons vous aider. Pour communiquer directement avec un auteur, consultez la première page de la revue dans laquelle son article a été publié afin de trouver ses coordonnées. Si vous n’arrivez pas à les repérer, communiquez avec nous à PublicationsArchive-ArchivesPublications@nrc-cnrc.gc.ca.

National Research Council Canada
Conseil national de recherches Canada

Laser-Ultrasonic Inspection of Cold Spray Additive Manufacturing Components

Daniel Lévesque, Christophe Bescond and Cristian Cojocaru

National Research Council Canada, Boucherville (Qc), Canada

Corresponding Author: daniel.levesque@cnrc-nrc.gc.ca

Abstract: Cold spray is a solid state coating technology with high deposition rates that is very suitable for large scale applications of additive manufacturing (AM). For quality control of complex parts, laser ultrasonics is particularly attractive due to its non-contact nature and is well adapted to online implementation. In this study, various inspection results performed off-line on metallic parts produced by the cold spray AM process are presented. Laser ultrasonics combined with the synthetic aperture focusing technique (SAFT) is used to detect flaws and through-thickness distributed porosity is investigated using the laser-ultrasonic backscattered signal. Also, laser shockwave is used to characterize bond strength at the interface between the deposition and the substrate. For post heat treatment of cold spray AM metallic parts, laser ultrasonics is used to monitor in real time recrystallization and sintering. Inspection results from either the top layer or the underside of the substrate are reported and discussed.

INTRODUCTION

The additive manufacturing (AM) process for metallic parts is an important emerging technology. In comparison to other AM processes, cold spray is differentiating as a solid state, high build rate, large scale deposition process [1-4]. As shown in Fig. 1 reproduced from Ref. [5], 1-100 µm powder particles are injected in a heated compressed gas (usually nitrogen, helium or a mixture of these 2 gases) flow that passes through a converging-diverging DeLaval type nozzle. While expanding in the diverging section of the nozzle, the gas will accelerate the particles to very high velocity (300-2200 m/s). Upon impact with a substrate the particles deform at very high strain rates, building a coating through this consolidation process. In contrast to other high temperature deposition processes, particles remain at the solid state all over the coating formation. This brings significant technological advantages such as: low residual stresses in the deposited material; very low oxidation level of the material although cold spray is carried out in open-atmosphere; potential to conserve metastable feedstock structures upon coating formation. As illustrated in Fig. 2, cold spray benefits from high deposition rates and that makes this process very suitable for large scale AM applications. Examples of use include part reinforcement and consolidation, advanced mold and die fabrication, rapid prototyping, dimensional restoration and structural repair.

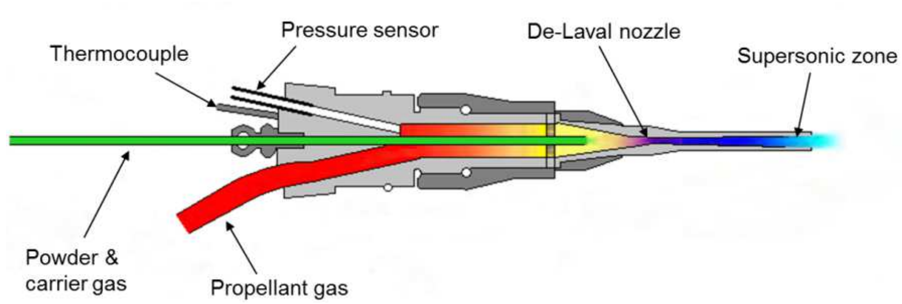

FIGURE 1. The principle of cold spray system (reproduced from Ref. [5]).

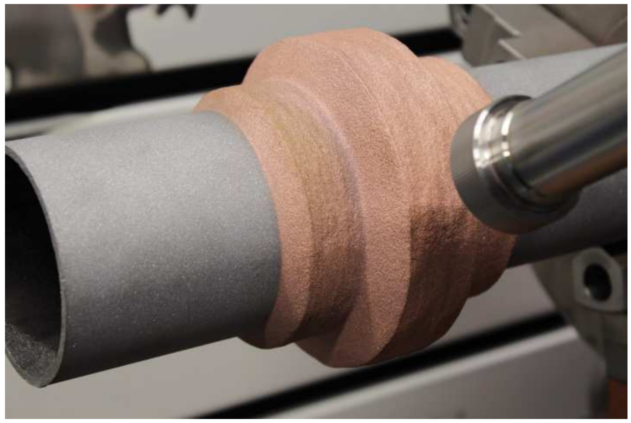

FIGURE 2. Illustration of cold spray AM process: 3 kg of Cu deposited in 20 min.

As a new technology in its early days before widespread acceptance, R&D efforts are required to improve, optimize and certify the process and the parts. In additive manufacturing process, components are built up layer by layer, which allow one to manufacture highly complex structures including walls, hollows to reduce weight, or internal fluid or gas channels. Quality control of such complex parts is a challenge and new strategies have to be developed [6]. For this purpose, laser ultrasonics is particularly attractive due to its non-contact nature and is well adapted to online implementation during the AM process [6, 7]. In a previous work, results obtained on INCONEL® 718 and Ti-6Al-4V coupons that were manufactured using laser powder, laser wire, or electron beam wire deposition were reported [8]. Defects such as lack of bonding, lack of fusion and discrete porosity were clearly detected and confirmed by X-ray micro-computed tomography (X-ray μCT). Regarding the cold spray AM process, a recent work investigated various nondestructive evaluation (NDE) methods including optical profilometry, eddy current and ultrasound for a set of NiCr on 304SS cold spray samples [9]. Distributed porosity, caused by improper process conditions such as temperature, gas velocity, spray parameters, powder size and surface cleanliness, was identified as the primary indicator of cold spray quality. Immersion focused ultrasound was used and attenuation showed some correlation with the porosity level.

In this study, various inspection results performed off-line on metallic parts produced by the cold spray AM process are presented. Laser ultrasonics is used to detect flaws using the synthetic aperture focusing technique (SAFT) [10], and through-thickness distributed porosity is investigated using the backscattered signal [11]. The latter approach was applied in recent years to study porosity in composite materials [12], as well as grain shape and size distribution in steel [13-15]. Also, laser shockwave technique is used to characterize bond strength [16, 17] at the interface between the cold spray deposition and the substrate. Finally, for the post heat treatment of cold spray AM metallic parts, laser-ultrasonic measurement can be performed to follow the recrystallization and sintering phenomena. Inspection results from either the top layer or the underside of the substrate are discussed.

LASER-ULTRASONIC INSPECTION FOR FLAW DETECTION

Laser ultrasonics combined with SAFT is first considered for flaw or porosity detection in cold spray samples. A set of three Al on Al cold spray samples intentionally manufactured with conditions to produce different porosity levels were prepared. Figure 3 shows one such sample. Sample #1 (8.8 mm thick coating) has a low porosity, sample #2 (5.5 mm thick coating) has an intermediate porosity and sample #3 (4.1 mm thick coating) has a high porosity with possible flaws present. Each coating is deposited on an Al 4.8 mm thick substrate.

For use with SAFT, the generation and detection zones overlapped at the surface for 1D or 2D scanning from either the top deposited layer or the underside of the substrate. Ultrasound generation was performed in the slight ablation regime (less than 1 μm) with a short pulse Nd:YAG laser in its 2^{nd} harmonic (532 nm wavelength) to achieve high frequencies. For detection, a long pulse Nd:YAG laser (1064 nm wavelength) and a small spot size were used. The phase demodulator was a 1-m long confocal Fabry-Perot interferometer in reflection mode. Frequency content up to 80 MHz was successfully generated and detected in the above test samples. Mechanical scanning along single lines up to 30 mm long was performed for data acquisition of the waveforms with a step size of 0.1 mm. SAFT reconstruction was performed with an aperture angle of 30º and a frequency bandwidth from 1.5 to 80 MHz using the longitudinal mode.

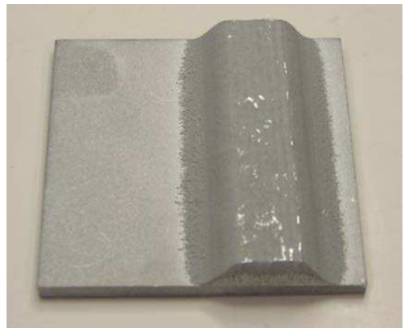

FIGURE 3. Photo of one Al/Al cold spray sample used for testing.

Using the above test conditions, line scans were performed on the underside of the substrate of the three samples over a length of 30 mm. B-scan images from the raw data and after SAFT reconstruction of a single scan line is shown in Fig. 4 for sample #2 of intermediate porosity, starting with the substrate on top. Weak indications are observed from the raw data image, some of them as hyperbola shapes, and they are more clearly resolved after SAFT reconstruction. The more or less continuous indications observed in Fig. 4b are attributed to the imperfect contact between layers associated with the multiple passes of the cold spray AM process. Also a strong indication of the substrate interface with the coating is apparent in both images. A similar indication of lower amplitude from the substrate is observed close to the last cold spray pass (bottom of B-scan), related to an echo propagating back and forth in the substrate. The longitudinal velocity difference between the Al substrate and the Al coating is small and such reflections are more related to the bond integrity of the coating with the substrate. This is also investigated further later in the paper.

Figure 5 shows a B-scan image after SAFT reconstruction of a particular scan line from the coating side over a length of 15 mm. As expected, the continuous indications attributed to the multiple passes are observed while a bit less resolved. Also the indication between last cold spray passes on top of the coating is missing due to the blind zone related to the large surface displacement in laser-ultrasonic signals.

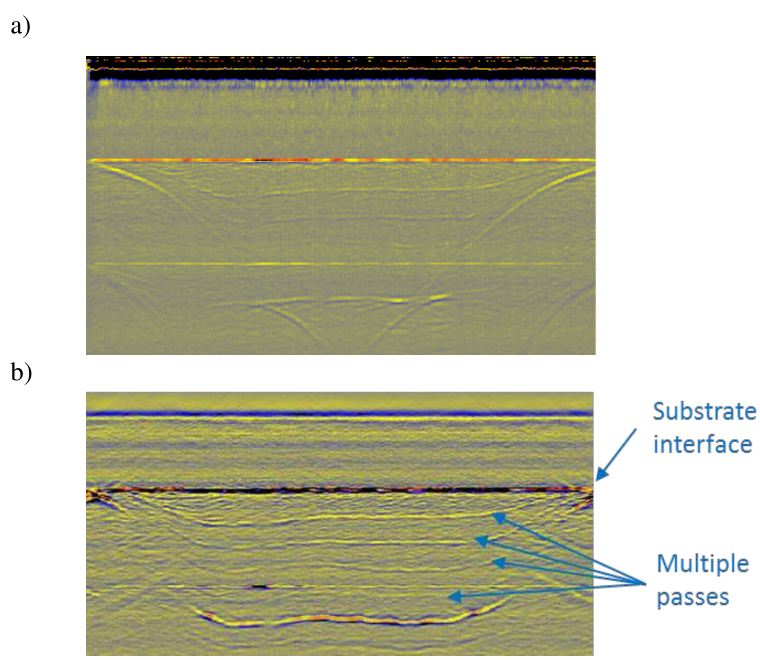

FIGURE 4. B-scans on Al/Al sample #2 from substrate, (a) raw data and (b) after SAFT reconstruction.

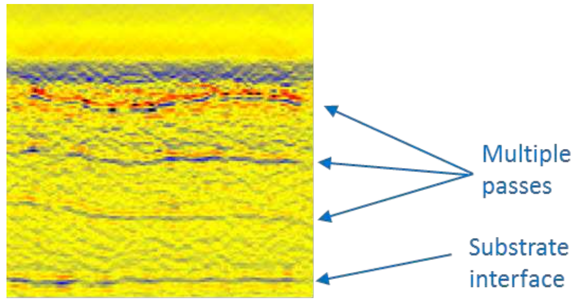

FIGURE 5. B-scans on Al/Al sample #2 from coating after SAFT reconstruction.

A further investigation was made on these samples using X-ray μCT as well as performing a series of micrographs. Figure 6a shows an X-ray μCT image after processing the radiographic data and Fig. 6b shows the series of micrographs concatenated in one picture. The agreement between the observations in these images and the laser-ultrasonic results is fairly good. From the micrograph image, porosity is present everywhere throughout the thickness, with a slightly larger pore concentration for the interface between each pass.

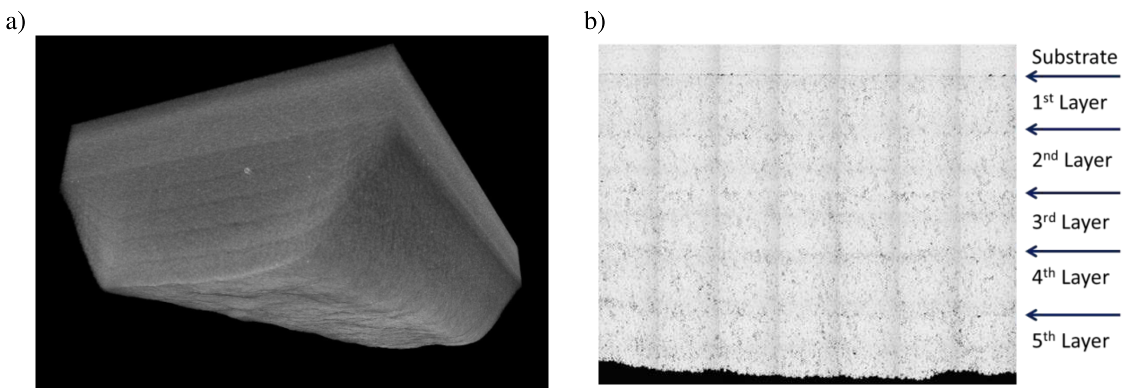

FIGURE 6. a) X-ray μCT image and b) concatenated micrographs for Al/Al sample #2.

LASER-ULTRASONIC BACKSCATTERING FOR POROSITY EVALUATION

To further study porosity, the spectral analysis of the laser-ultrasonic backscattered signals obtained from the top surface of the coating was considered. Figure 7 presents the principle of measurement with the backscattered amplitude (BSA) spectrum after averaging 100 spectra from a line scan, and the decay slope in the spectrum estimated between the two cursors. As shown in Fig. 7, the BSA method can be applied over the full time window between the large surface displacement and the first interface echo arrival, as an indication of average porosity found through the sample thickness. Figure 8 presents the correlation found between the BSA decay slope and average porosity in this limited set of Al/Al cold spray samples. In a further study, an analytical model for backscattering [12, 13] could be developed to relate such decay slope with the porosity level.

Additionally, a sliding small time window of typically 0.6 μs can be applied in the same time interval to estimate the decay slope in successive BSA spectra. Using the single scattering hypothesis, the time window location can be associated to an equivalent depth, where the BSA decay slope indicative of local porosity is estimated. Figure 9 shows the BSA decay slope as a function of depth and Fig. 10 shows the series of micrographs analyzed through the thickness of the three Al/Al cold spray samples. Compared to micrographs, consistent results are found between samples as well as through the thickness of each sample, with a larger negative slope corresponding to higher porosity near the top surface and a decreasing slope toward the substrate interface. Not shown here, an opposite behavior (smaller to larger negative slope) is found scanning from the substrate side and analyzing backscattered signals after the interface echo.

a) b)

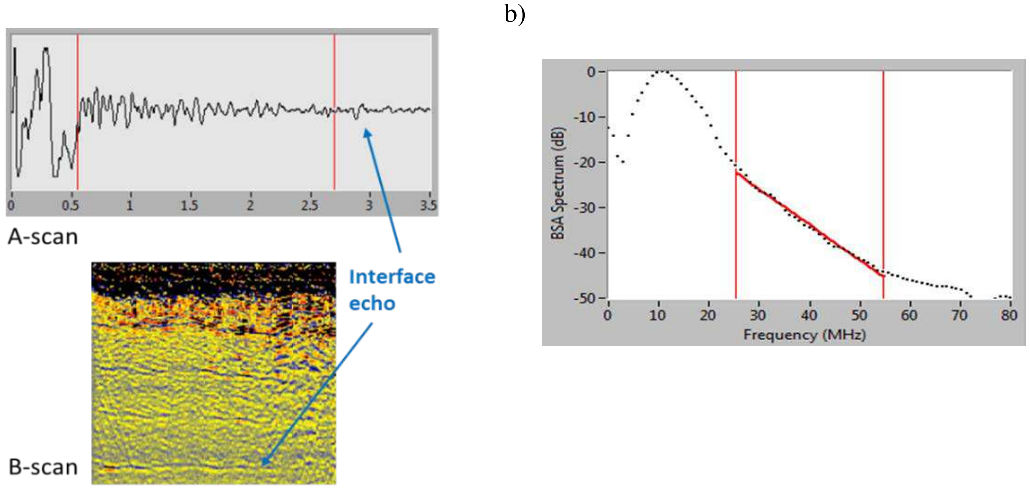

FIGURE 7. Principle of the BSA method used. Example of a) backscattered signal and b) BSA spectrum after averaging and decay slope estimated between the cursors.

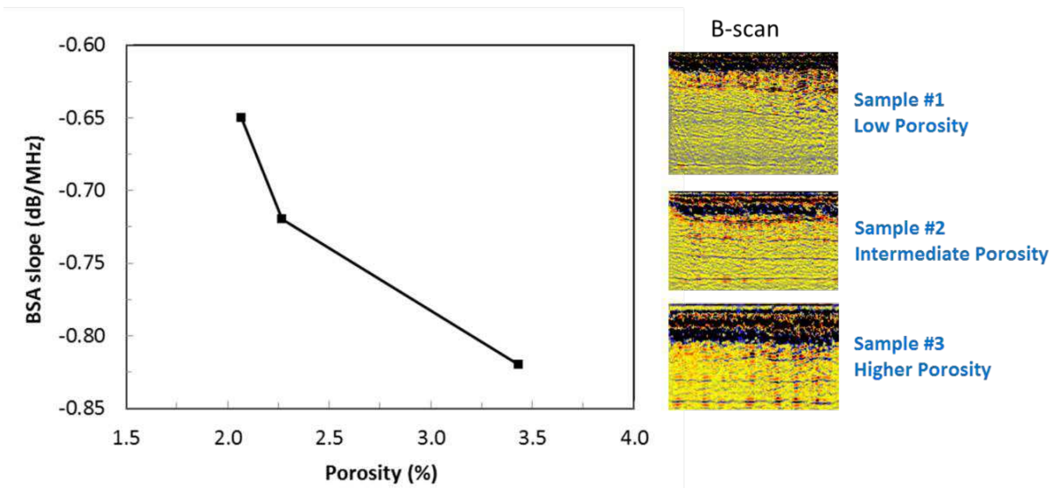

FIGURE 8. BSA decay slope as a function of through thickness average porosity, and corresponding B-scans in the Al/Al samples.

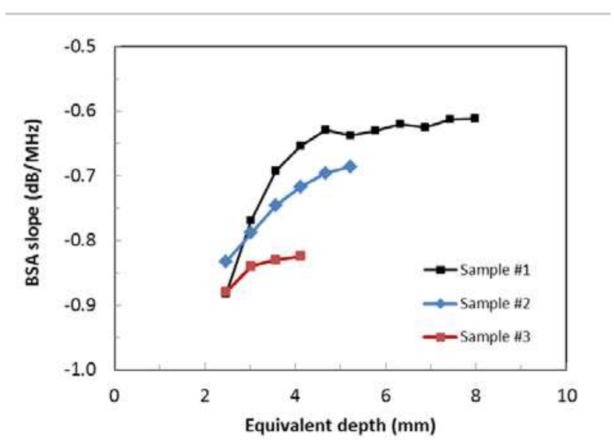

FIGURE 9. BSA decay slope as a function of depth through the thickness of the Al/Al samples.

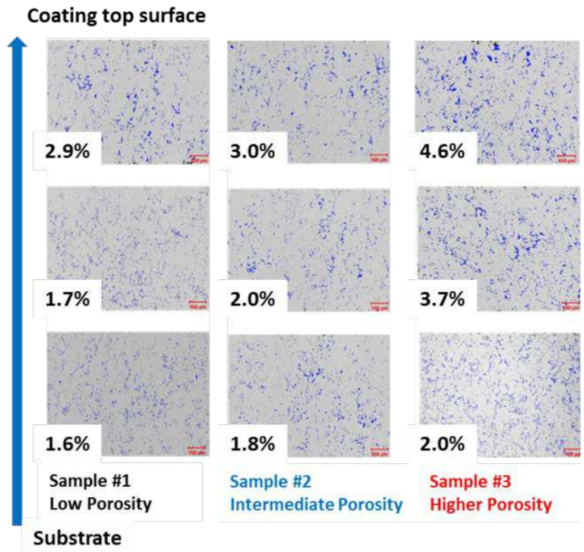

FIGURE 10. Series of micrographs through the thickness of the Al/Al samples.

While tested on a limited set of samples, the approach appears promising and will be further investigated. The method should work better when porosity near the surface is not too large to avoid strong reduction of the BSA signal deeper in the material. Also, the effect of multiple scattering should make the method not working well typically more than 4-5 mm deep.

LASER ULTRASONICS / SHOCKWAVE FOR BOND INTEGRITY ASSESSMENT

Another aspect to be considered with the cold spray AM process is the bond integrity between the coating and the substrate. This is particularly important for AM applications such as part reinforcement, dimensional restoration and structural repair. For these tests, a set of Al/Al cold spray samples were prepared with a pulsed laser surface pre-treatment to improve the adhesion between the coating and the substrate [18].

Line scans were performed on the underside of the substrate of the cold spray samples over a length of 42 mm. B-scan images after SAFT reconstruction of a single scan line of 4 samples is shown in Fig. 11, starting with the substrate on top. A clear indication of the substrate interface with the coating is apparent in all cases but of variable amplitude. As in Fig. 4b, such reflections should be related to the bond integrity and may vary depending on the surface treatment during the AM process. Also, there is a need to quantitatively determine the bond strength at the interface in each case.

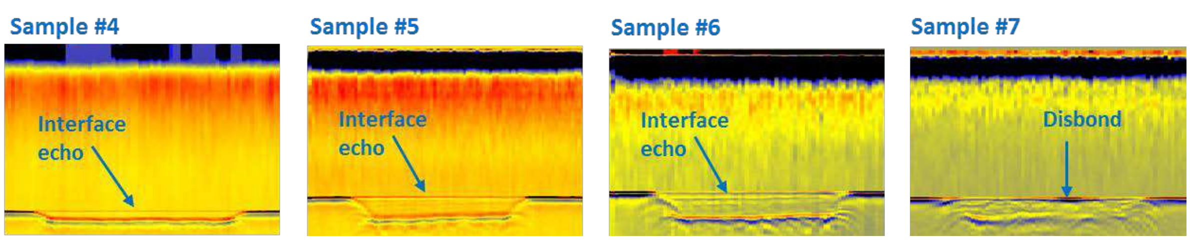

FIGURE 11. B-scans from substrate on the Al/Al samples with surface treatment after SAFT reconstruction.

For this purpose, a laser shockwave proof test method is considered with the principle shown in Fig. 12. With this technique, a high-energy pulsed laser produces a compressive large amplitude wave at the top surface of the sample. The compressive shock wave travels through the sample and after reaching the lower surface, the compressive wave is changed by the free surface into a tensile wave that travels back through the sample. A shock wave amplitude that reaches over a certain threshold will create tensile stresses large enough to debond interfaces in the component. By measuring the back surface velocity response with a Fabry-Perot etalon (velocimeter) [19] for different laser energy and using a model for shock wave propagation [20], the stress required to delaminate the coating from the substrate can be assessed. Figure 13 shows an example of such calculation for one of the cold spray samples. Calculated stress values are generally larger than in quasi-static mechanical tests since laser shock wave measurement involves high strain rate, typically of 10^5-10^6 s^{-1}. To confirm that the system debonded the interface, a post shock laser-ultrasonic inspection is used to perform C-scan imaging of the sample. The debonded interface will keep the ultrasound from propagating to the backside of the sample and this will be captured in the resulting image.

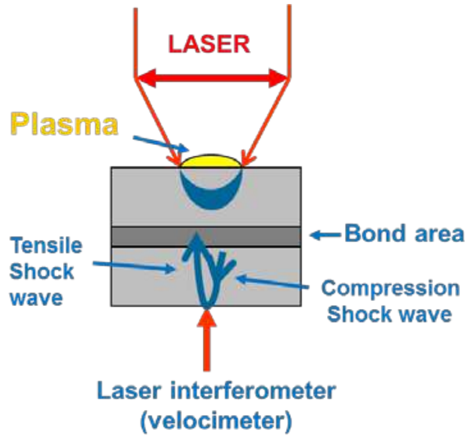

FIGURE 12. Principle of the laser shockwave proof test.

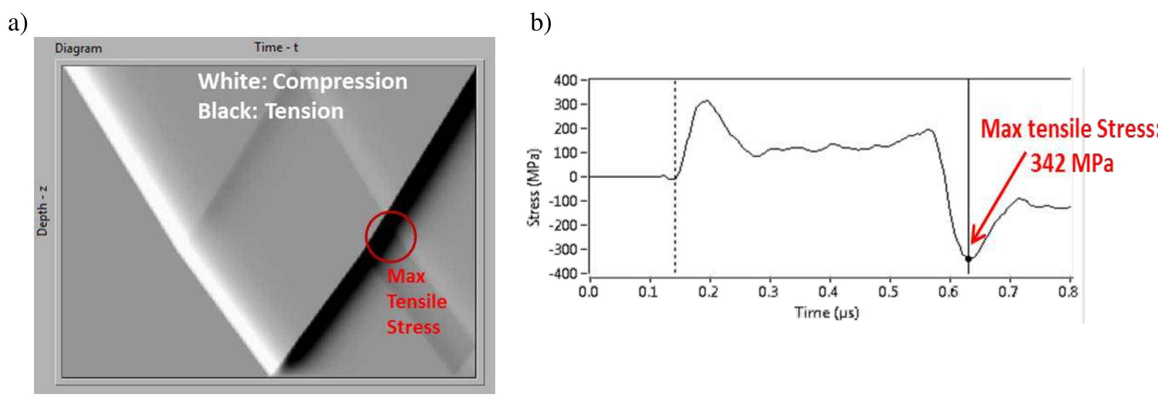

FIGURE 13. Example of a) ray tracing shock calculation with time-depth representation and b) stress evaluated at the interface from measured back surface velocity.

To determine bond strength, the laser shockwave technique was applied on the cold spray AM samples #4-6 not presenting a disbond in Fig. 11. Laser energies from 0.2 to 2.2 J were tested at different locations from the substrate side of each sample. Figure 14 shows the back surface velocity from the velocimeter (on the coating) at the different laser energies (indicated on right of each graph) and the post shock laser-ultrasonic C-scans on these samples. For sample #6, the bond did not opened for the laser energies tested. The back surface velocity response at the threshold laser energy producing a disbond is then used to calculate stress at the interface. Stress values calculated for corresponding laser energy breakage are given in Table 1. A more precise bond strength value could be obtained by testing each sample with more energy levels, but it may also vary from one location to another in the component.

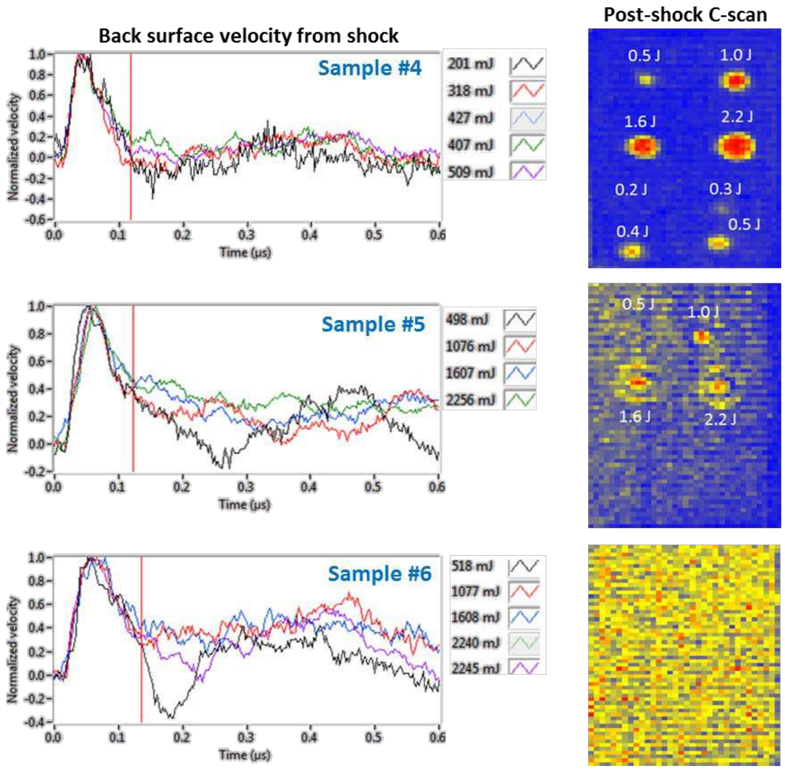

FIGURE 14. Back surface velocity at different laser energies and post shock laser-ultrasonic C-scans of the Al/Al samples.

TABLE 1. Calculated stress near breakage at the interface of the Al/Al samples.

Al/Al Sample ID	Coating thickness (mm)		Breakage energy (J)	Min Stress (MPa)	Max Stress (MPa)
4	0.7		0.3	104	242
5	0.9		0.5	271	393
6	1.2		2.2+	358	N/A

LASER-ULTRASONIC MONITORING DURING HEAT TREATMENT

In some applications of cold spray AM process, a post heat treatment of the component is required. Laser-ultrasonic monitoring can be performed at high temperature during such heat treatment to better understand and optimize the occurrence of recrystallization and sintering. As a first study, cold spray samples made of H13 tool steel on mild steel substrate were prepared. Then, the 3.3 mm thick H13 coating of each sample was detached from the substrate and inserted in a Gleeble machine for direct resistance heating. A laser-ultrasonic system coupled with the Gleeble was used to monitor the longitudinal velocity as function of time and temperature. Such a system was developed in the past to study grain size evolution and phase transformation in steel [14, 15, 21]. Two different heat treatments are considered for these tests.

Figure 15 shows the temperature history for the first heat treatment of long duration and corresponding ultrasonic velocity as function of temperature on a stand-alone H13 sample. The ultrasonic velocity for the cold spray sample starts with a quite low value of 4.5 mm/µs and reaches 6.0 mm/µs after such heat treatment, as expected for bulk H13 tool steel. Moreover, the ultrasonic velocity exhibits two changes in its behavior near 550ºC and later at 800ºC. These changes are found attributable as a clear effect of recrystallization and sintering, respectively.

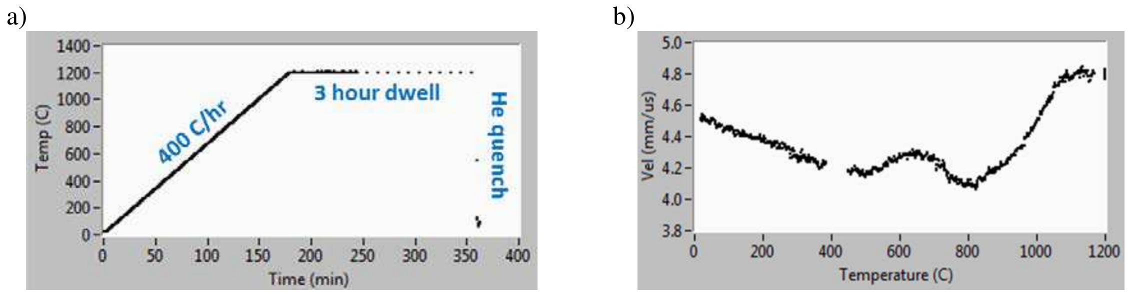

FIGURE 15. a) Temperature history of first heat treatment and b) ultrasonic velocity as function of temperature.

Figure 16 shows the temperature history and ultrasonic velocity for the second heat treatment of short duration on another stand-alone H13 sample. Again, the ultrasonic velocity starts with a low value of 4.5 mm/μs and reaches only 5.5 mm/μs during the slow cooling phase of this heat treatment. Also, the ultrasonic velocity during heating shows a dynamic behavior quite different than in the previous case and this remains to be further investigated.

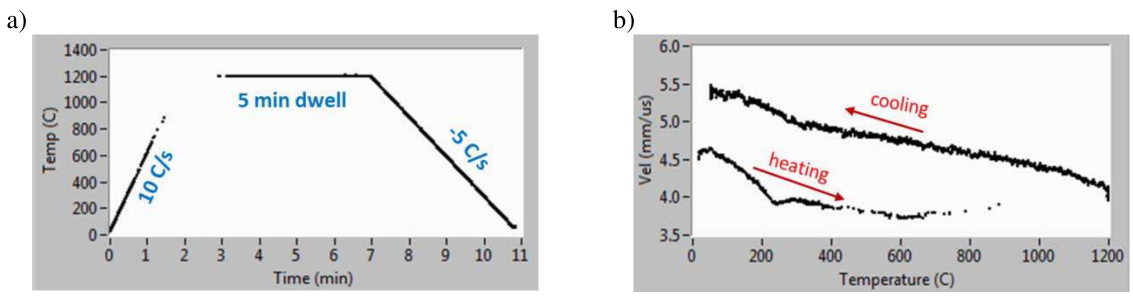

FIGURE 16. a) Temperature history of second heat treatment and b) ultrasonic velocity as function of temperature.

CONCLUSION

Several aspects were considered in this paper regarding the laser-ultrasonic inspection of cold spray AM components. Laser ultrasonics combined with SAFT was used to detect flaws in Al/Al samples from the substrate and from the deposition. Indications of multi-passes and variations in bond integrity with the substrate were observed. This was further validated by X-ray μCT and a series of micrographs showing larger pore concentration between each pass.

Another aspect was considering through-thickness distributed porosity using a spectral analysis of the laser-ultrasonic backscattered signal. A fairly good correlation is found between the BSA decay slope and average porosity in the set of Al/Al samples tested. Using a sliding time window, the BSA decay slope was found promising to provide indication of porosity variations through the sample thickness as confirmed by a series of micrographs.

Also, the laser shockwave technique was used to characterize bond strength at the interface between the cold spray deposition and the substrate. Finally, for the post heat treatment of cold spray AM metallic parts, laser-ultrasonic measurement was shown to be useful to monitor the recrystallization and sintering phenomena.

ACKNOWLEDGMENTS

This work has been conducted within the NRC's Cold Spray Additive Manufacturing Industrial R&D Group. The authors are grateful to J.-G. Legoux for the fruitful discussion in the interpretation of results, to M. Zieman and D. de Lagrave for their contribution in the sample preparation and performing the series of micrographs, as well as to C. Brosseau and M. Lord for their participation in the laser-ultrasonic measurements of the cold spray samples tested in this work.

REFERENCES

1. E. Irissou et al., "Review on Cold Spray Process and Technology: Part I---Intellectual Property", *J. Thermal Spray Technol.*, **17**, pp. 495-516 (2008).
2. Wang et al., "Characterization and modeling of the bonding process in cold spray additive manufacturing", *Additive Manufacturing*, **8**, pp. 149-162 (2015).
3. Yin et al., "Cold spray additive manufacturing and repair: Fundamentals and applications", *Additive Manufacturing*, **21**, pp. 628-650 (2018).
4. Li et al., "Solid-state additive manufacturing and repairing by cold spraying: A review", *J. Mater. Sci. & Technol.*, **34**, pp. 440-457 (2018).
5. D.K. Christoulis, M. Jeandin, E. Irissou, J.-G. Legoux and W. Knapp, "Laser-Assisted Cold Spray (LACS)", Chapter 5 in Nd:YAG Laser", ISBN: 978-953-51-0105-5, D.C. Dumitras Ed. Intech, 2012, pp. 59-96
6. S.K. Everton et al., "Review of in-situ process monitoring and in-situ metrology for metal additive manufacturing", *Materials and Design,* **95**, pp. 431-445 (2016).
7. S. Everton, P. Dickens, C. Tuck, B. Dutton, "Evaluation of laser ultrasonic testing for inspection of metal additive manufacturing", *in Proceedings, Laser 3D Manufacturing II*, 2015, edited by H. Helvajian, A. Piqué, M. Wegener, B. Gu, (Proc. of SPIE Vol. 9353, 2015), 935316.
8. D. Lévesque, C. Bescond, M. Lord, X. Cao, P. Wanjara, J.-P. Monchalin, "Inspection of additive manufactured parts using laser ultrasonics", *in Proceedings, 42nd Annual Review of Progress in Quantitative Nondestructive Evaluation*, Minneapolis, MN, 2015, edited by D.E. Chimenti, L.J. Bond, (AIP Conf. Proc. 1706, 2016), 130003.
9. S.W. Glass, M.R. Larche, M.S. Prowant, J.D. Suter, J.P. Lareau, X. Jiang, and. K.A. Ross, "Cold spray NDE for porosity and other process anomalies", *in Proceedings, 44th Annual Review of Progress in Quantitative Nondestructive Evaluation,* Provo, UT, 2017, edited by D.E. Chimenti, L.J. Bond, (AIP Conf. Proc. 1949, 2018), 020010.
10. D. Lévesque, A. Blouin, C. Néron, J.-P. Monchalin, *Ultrasonics,* **40**, pp. 1057-1063 (2002).
11. S.E. Kruger, A. Moreau, D. Lévesque, M. Lord, "Laser ultrasonic measurements of scattered waves in steel", *in Proceedings, Review of Progress in Quantitative Nondestructive Evaluation Vol. 20*, edited by D.O. Thompson and D.E. Chimenti, pp. 1298-1305, 2001.
12. A.A. Karabutov, N.B. Podymova, "Nondestructive porosity assessment of CFRP composites with spectral analysis of backscattered laser-induced ultrasonic pulses", *J. Nondestr. Eval.,* **32**, pp. 315-324 (2013).
13. O.I. Lobkis, L. Yang, J. Li, S.I. Rokhlin, *Ultrasonics,* **52**, pp. 694-705 (2012).
14. N. Legrand et al., "Laser-ultrasonic sensor to monitor steel microstructure at elevated temperature: Applications to hot rolling", *in Proceedings, 4th International Symposium on Laser Ultrasonics and Advanced Sensing (LU2015)*, Evanston, IL, 2015, paper #53.
15. D. Lévesque, "Laser-ultrasonic methods to characterize steel microstructure: Overview and recent developments", *3rd International Workshop on Laser-Ultrasound for metals*, Stockholm, Sweden, 2017.
16. J. L. Vossen, "Measurements of film – substrate bond strength by laser spallation." *ASTM Spec. Tech. Publ. Am. Soc. Test. Mater.*, **640,** pp. 122–133 (1978).
17. V. Gupta, et al, "Measurement of interface strength by laser-pulse-induced spallation", *Mater. Sci. Eng*., **A 126**, pp. 105–17 (1990).
18. D.K. Christoulis et al., "Cold-Spraying Coupled to Nano-Pulsed Nd-YaG Laser Surface Pre-treatment", *J. Thermal Spray Technol.*, **19**, pp. 1062-1073 (2010).
19. M. Arrigoni, et al., "Laser Doppler interferometer based on a solid Fabry-Perot etalon for measurement of surface velocity in shock experiments," *Meas. Sci. Technol.*, **20**, 015302 (2009).
20. M. Perton, D. Lévesque, J.-P. Monchalin, M. Lord, J.A. Smith, and B.H. Rabin, "Laser shockwave technique for characterization of nuclear fuel plate interfaces", *in Proceedings, 39th Annual Review of Progress in Quantitative Nondestructive Evaluation*, Denver, CO, 2012, edited by D.O. Thompson and D.E. Chimenti, (AIP Conf. Proc. 1511, 2013), pp. 345-352.
21. S.E. Kruger, E.B. Damm, *Mater. Sci. and Eng.,* **A 425**, pp. 238-243 (2006).